Rare Metal Materials and Engineering
Volume 55, Issue 4, April 2026
Available online at www.rmme.ac.cn

Science Press

Cite this article as: Huang Wenzhan, Liu Tao, Chen Yao, et al. Influence of SiC Content on Foaming Stability, Cell Structure, and Compression Performance of SiC/Al-Based Composite Foam Prepared by Two-Step Foaming Method[J]. Rare Metal Materials and Engineering, 2026, 55(04): 890-898. DOI: https://doi. org/10.12442/j.issn.1002-185X.20250062.

ARTICLE

Influence of SiC Content on Foaming Stability, Cell Structure, and Compression Performance of SiC/Al-Based Composite Foam Prepared by Two-Step Foaming Method

Huang Wenzhan, Liu Tao, Chen Yao, Wang Lucai, Wu Jianguo, You Xiaohong

School of Materials Science and Engineering, Taiyuan University of Science and Technology, Taiyuan 030024, China

Abstract: SiC/Al-based composite foams were prepared by a two-step foaming method. The influence of the SiC content and its distribution uniformity on the foaming stability, cell structure, and mechanical properties of the aluminum foams was investigated. The macro/micro-features of the aluminum foams were characterized and analyzed. Results demonstrate that an appropriate increase in SiC content and the uniform distribution of SiC can improve the foaming stability, optimize the cell diameter and cell wall thickness, ameliorate the cell distribution, and enhance the hardness and compressive strength of the aluminum foams. However, either insufficient or excessive SiC leads to uneven distribution of SiC particles, which is unfavorable to foaming stability and good cell structure formation. With 6wt% SiC, both the foaming stability and cell structure of the aluminum foam reach the optimal state, resulting in the highest compressive strength and optimal energy absorption capacity.

Key words: aluminum foam; two-step foaming method; foaming stability; cell structure; hardness; compressive strength

1 Introduction

Aluminum foam has potential applications in aerospace, automobile, and construction because of its light mass, high strength, and exceptional acoustic and energy absorption properties[1–4]. García-Moreno et al[5] reported that the commercial production of aluminum foam by the melt metallurgy method has been conducted since the 1980s. A series of methods have been proposed for the preparation of aluminum foams, mainly including the melt foaming method, powder metallurgical foaming method, and gas injection foaming method[6]. Among them, the two-step foaming method, as an improved melt foaming method, has been widely studied due to its advantages of simple process, low cost, and the ability to prepare aluminum foams with specific configurations[7–9].

It is well known that the preparation of aluminum foam by the two-step foaming method is affected by numerous factors, such as the type and content of reinforcement particles[10–12]. The selection of suitable reinforcement particles can significantly optimize the cell morphology and enhance the stability of aluminum foam[13–14]. Lin et al[15] found that the stability of aluminum foam could be effectively improved by adding SiC particles and magnesium powder. However, Kumar et al[16] enhanced the stability and swelling property of aluminum foam by adding $AlMgO_2$ particles. In addition, ZrB_2 particles were used as stabilizing particles for aluminum foam[17], which could optimize the cell structure and swelling property of aluminum foam. These studies indicate that the addition of reinforcement particles can significantly improve the stability of aluminum foam. Aluminum foam is widely used in impact cushioning devices due to its excellent mechanical and functional properties. However, the relatively low platform stress restricts its wider application. Therefore, enhancing the mechanical properties of aluminum foam has

Received date: April 08, 2025
Foundation item: Doctoral Startup Fund (20192066, 20212028); Laijin Excellent Doctoral Fund (20202021); Scientific and Technological Innovation of Colleges and Universities in Shanxi Province (2020L0342); Fundamental Research Program of Shanxi Province (202303021222178)
Corresponding author: Huang Wenzhan, Ph. D., Professor, School of Materials Science and Engineering, Taiyuan University of Science and Technology, Taiyuan 030024, P. R. China, E-mail: 2019063@tyust.edu.cn

become one of the research priorities. Sinha et al[18] improved the platform stress and mechanical properties of aluminum foam by incorporating graphene flakes into the precursor. Mudge et al[19] used novel Al-TiH_2 epispastic precursor particles to prepare aluminum foam with uniform cell distribution and enhanced energy absorption. Similarly, the enhancement of the platform stress and energy absorption values of aluminum foams can be achieved through the γ-Al_2O_3 nanostructures and SiC particle enhancement[20–21]. Ad-ditionally, the toughness and bending properties of aluminum foams were also improved to expand the applications of aluminum foams[22–23].

The effects of different additives on the microstructure and energy absorption of aluminum foams have been widely researched. However, the information about optimizing the content of SiC additives is insufficient to improve the mechanical properties of aluminum foams by the two-step foaming method. The studies on the homogeneity of internal cells and related mechanisms of property changes of aluminum foams also attract much attention. In this study, the aluminum foam with good foaming stability, cell structure, and mechanical properties were prepared by adjusting the SiC content using the two-step foaming method. The average cell diameter, cell wall thickness, cell distribution, hardness, and compression properties of the samples were investigated and analyzed, revealing the influence of SiC content on the microstructure and mechanical properties of the aluminum foams. This research provides a reference for the further design of aluminum foam with optimized cell structure and enhanced mechanical properties.

2 Experiment

Fig. 1 shows the process flow for the preparation of aluminum foam precursors. In this research, ZL102 aluminum alloy was used as the matrix material. 1.5wt% TiH_2 was used as the foaming agent, and 1wt%, 2wt%, 3wt%, 4wt%, 6wt%, and 8wt% SiC was used as the thickener. Firstly, the ZL102 aluminum alloy was heated to melting state at 660 °C. Then, the SiC powder, which was heated at 700 °C for 2 h, was added to the aluminum melt and stirred for 5 min to ensure a homogenous distribution of SiC. Subsequently, the temperature was reduced to 610 °C, and the pre-treated TiH_2 powder was added to the aluminum melt and stirred for 90 s to ensure uniform dispersion. Finally, the melt was rapidly poured into a mold for quick solidification. After demolding, the aluminum foam precursor was obtained.

Fig. 2 shows the process flow of the preparation of aluminum foams. Before foaming, the molds needed to be preheated at 660–720 °C for 30 s to ensure that their temperature reached the foaming temperature. Then, the sample was placed in the mold and kept in the furnace for thermal foaming. After the foaming was completed, the mold was removed and slowly cooled. Finally, after demolding, the aluminum foam was obtained.

Cylindrical samples of Φ20 mm×20 mm were prepared from the aluminum foams with SiC content of 1wt%, 2wt%, 3wt%, 4wt%, 6wt%, and 8wt% at the foaming temperature of 680 °C using the wire cutting machine. After the samples were ground and polished, the sample surfaces were corroded with 5wt% NaOH solution. The cell structure parameters of the aluminum foam after binary processing were analyzed using the ImageJ software. The microstructure and composition of the samples were analyzed using a KEYENCE ultra-depth field optical microscope (OM), scanning electron microscope (SEM, ZEISS), and an energy dispersive spectrometer (EDS). The porosity and cell morphology of the samples were observed using computerized tomography (CT) technique. Lastly, the compression performance of the samples was tested using a universal testing machine. The sample porosity P_{foam} was measured by the Archimedes drainage method, which is expressed by Eq.(1):

$$P_{foam} = \left[1 - \frac{M_1\rho_0}{(M_1 - M_2)\rho_1}\right] \times 100\% \quad (1)$$

where ρ_0 represents the density of water (1 g/cm^3); ρ_1 is the density of the matrix material (1 g/cm^3); M_1 is the mass of the aluminum foam (g); M_2 is the mass of the aluminum foam after water is displaced (g). The calculation for the average cell diameter is expressed as follows:

$$\overline{D} = \frac{1}{N}\sum_{i=1,2}^{N} D_i \sqrt{\frac{\eta'}{n_i}} \quad (2)$$

where $\overline{D}$ represents the average cell diameter (mm); N is the number of sections; D_i is the diameter of the section (mm); η' is the area porosity (%); n_i is the number of cells per section. The calculation for the cell wall thickness is stated as follows:

$$\overline{M} = \left(0.9523\sqrt{\frac{1}{\eta'}} - 1\right)\overline{D} \quad (3)$$

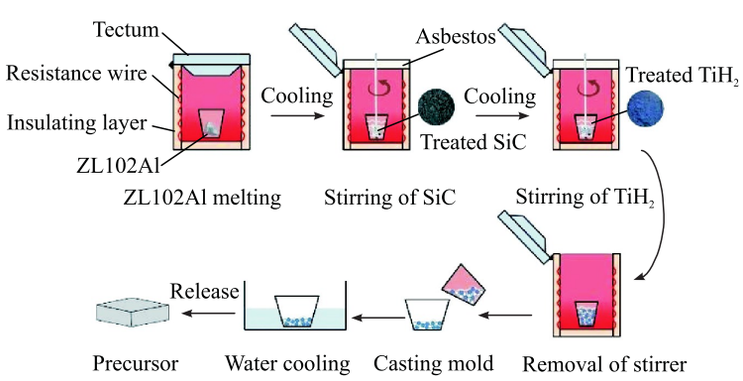

Fig.1 Process flow of preparation of precursors

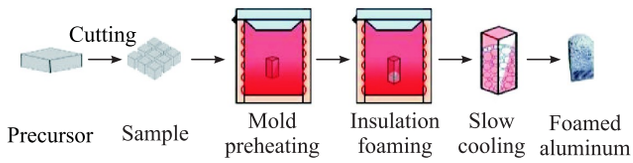

Fig.2 Process flow of preparation of aluminum foams

where $\overline{M}$ represents the cell wall thickness.

3 Results and Discussion

3.1 Influence of SiC content on foaming stability and macroscopic defects of aluminum foams

The appearances of aluminum foams with different SiC contents for different foaming time are shown in Fig.3. When the SiC content is 1wt%–4wt%, the aluminum foams have inferior consistency in cell wall thickness with obvious thin-thickness differences, varying sizes of cells, and irregular cell shapes. When the SiC content is 6wt%, the aluminum foam exhibits a good cell structure. The cell pattern is dominated by closed polygonal cells with thin uniform walls and large cell diameters. However, when the SiC content reaches 8wt%, a large number of large cells appear in the aluminum foam. This is mainly attributed to the change in melt viscosity. The increase in content of SiC improves the viscosity of the melt during the foaming process, which further strengthens the liquid-phase film[24–25]. Low-viscosity (1wt% – 3wt%) and transition-viscosity (4wt%) melts have a weak liquid-phase film, and the gas easily escapes, which is very unstable. Compared with the low-viscosity melt, the liquid-phase film in the appropriate-viscosity (6wt%) melt is more stable, and the gas is less likely to escape, which effectively inhibits the bubble rupture[26–27]. However, the high-viscosity (8wt%) melt inhibits the release of gas from the foaming agent as well as the excessive obstruction of cell growth, which leads to the prolongation of foaming time. With the prolongation of foaming time, the new cells expand, whereas the mature cells are over-expanded by a combination of heat and stress, eventually ruptured, and merged to form large cells (marked by green dashed circles in Fig.3). In addition, the non-uniform distribution of SiC promotes the generation of large cells.

To further investigate the foaming stability, the foaming time is prolonged by 10, 15, 30, 35, 60, and 60 s for the aluminum foams with 1wt%, 2wt%, 3wt%, 4wt%, 6wt%, and 8wt% SiC, respectively. With the prolongation of foaming time, the foams show decaying behavior, and the destruction of cell structure is obvious. The cell structure of aluminum foams at low- and transition-viscosity states is severely damaged in a short time, and a large number of connected cells (marked by yellow dashed circles in Fig. 3), deformed cells (marked by red dashed circles in Fig. 3), and large cells are formed, which increases the difficulty to prepare aluminum foams. Due to the increase in melt viscosity, the cell structure of aluminum foams at suitable- and high-viscosity states is slightly destroyed to a small extent. Therefore, the increase in SiC content enhances the melt viscosity during the foaming process, which promotes the foaming stability.

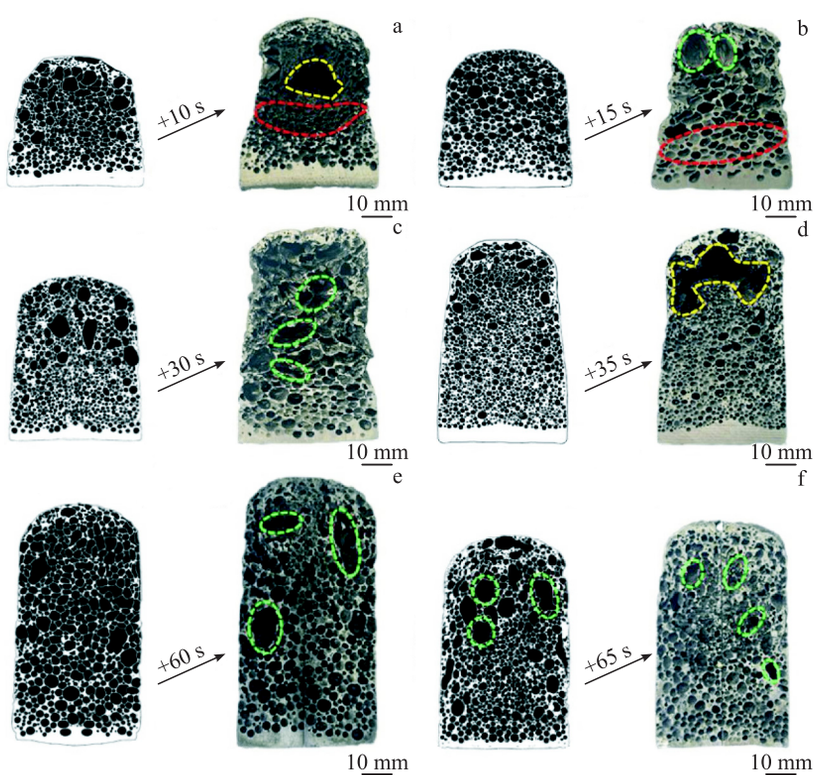

Fig.3 Appearances of aluminum foams with different SiC contents for different foaming time: (a) 1wt%, (b) 2wt%, (c) 3wt%, (d) 4wt%, (e) 6wt%, and (f) 8wt%

3.2 Microstructure analysis of aluminum foams

3.2.1 Analysis of SiC particle distribution in aluminum foams

Fig. 4 shows OM images of aluminum foams with 1wt%, 2wt%, 3wt%, 4wt%, 6wt%, and 8wt% SiC. Among them, numerous large-sized α-Al grains with irregular shapes are randomly distributed, and the SiC particles on the cell walls are surround by a large number of microcells in the aluminum foams with 1wt% – 4wt% SiC. This phenomenon is mainly attributed to the high stress gradient between the Al matrix and the SiC particles during the solidification of the melt due to the large difference in their coefficients of thermal expansion. To overcome this stress, the matrix undergoes tearing, leading to the formation of tiny cells, which ultimately affects the microstructure and properties of the material[28]. Notably, the α-Al grain size is significantly refined, and the size and number of microcells in the aluminum foam with 6wt% SiC decrease. In this case, the SiC particles are more uniformly distributed in the aluminum matrix, embedding themselves into most of the air cell interfaces. The mutual contact and friction behavior of the particles are intensified, and the slip is hindered. Additionally, the density of SiC particles increases, forming a tightly packed network. This phenomenon enables the aluminum matrix to form an effective reinforcing effect, enhances the hardness and strength of the aluminum foam[29], reduces the regional differences in the melt viscosity, and inhibits the aggregation and diffusion of the cells. The foaming stability of the cells is improved, thus enhancing overall mechanical properties. However, when the SiC content reaches 8wt%, large-sized clusters of SiC particles appear on the cell wall, leading to excessive local viscosity of the melt, which excessively hinders the cell growth and produces large cells in the local region, and deteriorating the overall foaming effect. Therefore, controlling the content of SiC particles is essential for adjusting the melt viscosity during the foaming process to obtain the aluminum foams with better microstructure.

3.2.2 Microstructure analysis of aluminum foam with 6wt% SiC

Fig.5 shows the microstructures and EDS analysis results of the aluminum foam with 6wt% SiC. There are tiny defective cells in the cell wall of the aluminum foam with 6wt% SiC, as shown in Fig. 5a, which are mainly located at the Prato boundary and cell interface. This structure may affect the compressive strength and toughness of the aluminum foam. The distribution of SiC particles, Al grains, and Al-Si eutectic pariticles shows that the SiC particles are dispersed in the Al-Si eutectic structure, and their pinning effect can effectively retard the decomposition of TiH_2 particles. Meanwhile, the uniform distribution of SiC particles in the matrix can increase the melt viscosity during the foaming process, effectively inhibit the condensation and rupture of the air holes, and achieve the high stability of foaming.

3.2.3 Vickers hardness variation in aluminum foams

Fig.6 shows the Vickers hardness variation in the regions of α-Al grains, Al-Si eutectic particles, and SiC particles of the aluminum foams with 1wt%, 2wt%, 3wt%, 4wt%, 6wt%, and 8wt% SiC. The results indicate that the increase in SiC content does not significantly affect the Vickers hardness of the α-Al region, but greatly increases the Vickers hardness of the SiC and Al-Si regions. Notably, the Vickers hardness of the SiC region is higher than that of the Al-Si region. The SiC particles effectively share the load as a reinforcing phase and play a positive role in improving the hardness of the aluminum foam[30]. After appropriately increasing the SiC content, the SiC particles with a large number and small size are more uniformly distributed in the aluminum melt, and the particle spacing becomes relatively smaller. These particles provide more slip resistance, effectively preventing the surface slip and enhancing the material strength. In addition, the uniform distribution of SiC particles in the cell wall of the aluminum foam hinders the crack expansion path, effectively

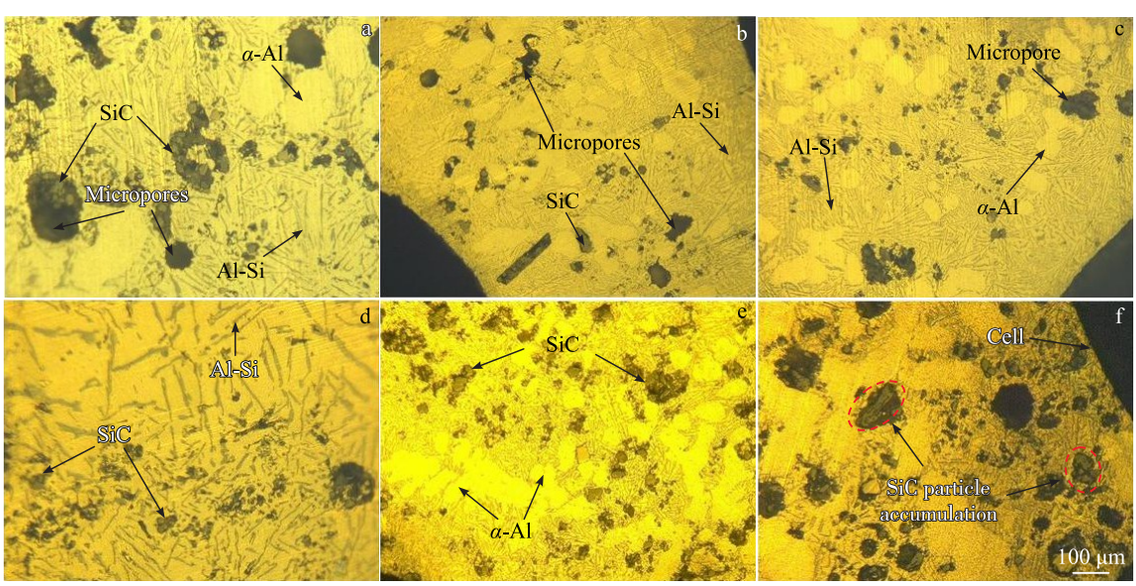

Fig.4 OM images of aluminum foams with different SiC contents: (a) 1wt%, (b) 2wt%, (c) 3wt%, (d) 4wt%, (e) 6wt%, and (f) 8wt%

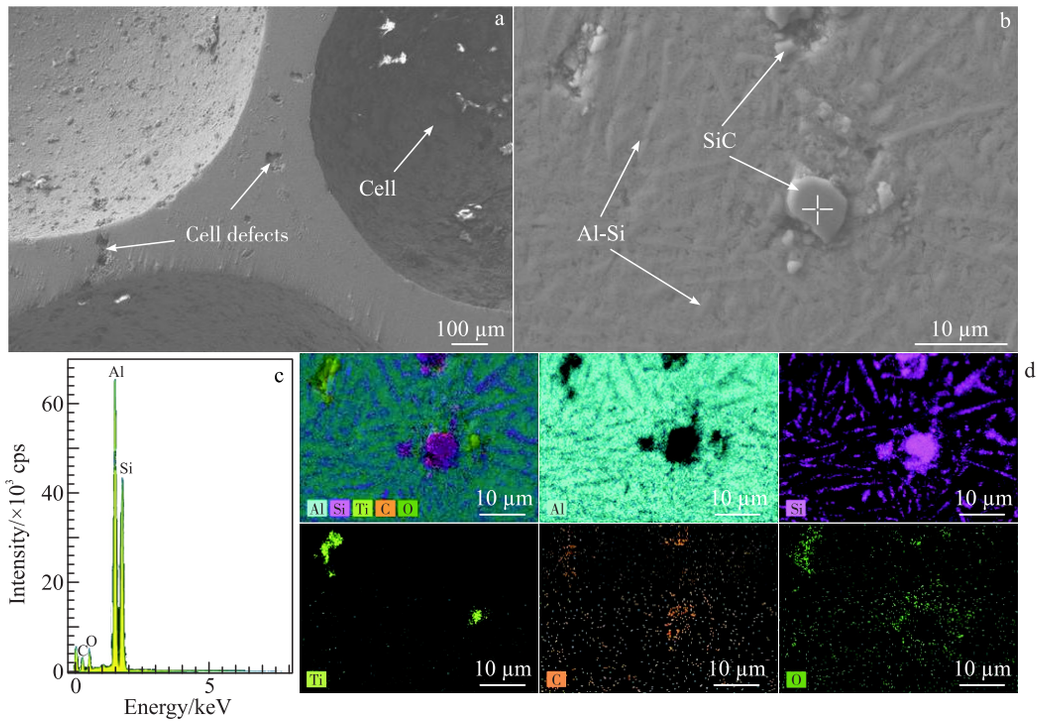

Fig.5 SEM images of 6wt% SiC aluminum foam (a – b); EDS analysis spectrum of point marked in Fig. 5b (c); EDS element distributions corresponding to Fig.5b (d)

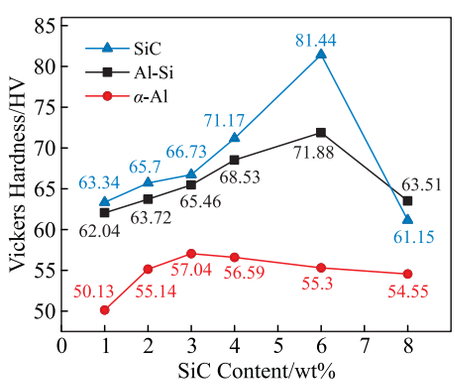

Fig.6 Vickers hardness variations in the regions of α-Al grains, Al-Si eutectic particles, and SiC particles of aluminum foams

preventing the crack expansion or reducing the crack expansion rate. Meanwhile, fine and elongated Al-Si eutectic particles are distributed in the aluminum matrix, and their uniform dense microstructure also contributes to the enhancement in hardness of aluminum foam. However, the clusters and aggregated bands of the SiC particles (Fig.4) lead to the formation of microcells, which reduces the bonding strength at the interface, thus preventing the effective transfer of loads and ultimately affecting the hardness of the aluminum foam.

In summary, it can be seen that the micro-properties of the aluminum foam matrix are significantly influenced by the distribution and content of the SiC particles. The influence of SiC particles on the aluminum foam matrix can be expressed by Eq.(4):

$$P_M = P_{ZL102} \pm \left(E_c + E_U\right) \quad (4)$$

where P_M is the property of the aluminum foam matrix; P_{ZL102} is the inherent property of the aluminum matrix without SiC particle addition; E_c is the influence of SiC content on the aluminum matrix; E_U is the influence of SiC particle distribution on the aluminum matrix. The uniformly distributed SiC particles optimize the Vickers hardness of the aluminum matrix and inhibit the crack diffusion. Adding a suitable number of SiC particles can enhance the Vickers hardness of the composite material. However, an excessively high content of SiC particles leads to particle accumulation, causing stress concentration, which deteriorates the material properties. In addition, the distribution and content of the SiC particles also have a significant influence on the stability of the aluminum foam cell structure[31], which can be expressed by Eq.(5–6), as follows:

$$E_U \propto E_c \quad (5)$$

$$Al_{fs} = E_U + E_c + E_s \quad (6)$$

where Al_{fs} represents the stability of the aluminum foam cell structure; E_s is the impact on the stability of the liquid-phase film. The addition of SiC increases the viscosity of the aluminum melt and decreases the cell growth rate. It also reduces the interfacial tension of the cells, enhances the stability of the liquid film, and reduces the merging and rupture phenomena of the cells. These effects jointly regulate the size and distribution of the cell and cell wall, resulting in a uniformly distributed supportive structure, which ultimately improves the stability of the cell structure.

3.3 Influence of SiC content on cell structure of aluminum foams

3.3.1 Influence of SiC content on average cell size and cell wall thickness of aluminum foams

Fig. 7 shows the changes in the average cell size and cell wall thickness of the aluminum foams with different SiC contents. From the variation of the average cell size, when the SiC content is less than 4wt%, the average cell size of low-viscosity aluminum foam shows a decreasing trend with the increase in SiC content. This indicates that the hindering effect caused by increasing viscosity on bubble growth is more significant than the promotion effect caused by the uniform distribution of SiC particle. Notably, the average cell size of the aluminum foam increases when the SiC content increases from 4wt% to 6wt%. This is attributed to the more uniform distribution of SiC particles, which provides a more stable liquid-phase film. In this case, the promotion effect of bubble growth caused by the uniform distribution of SiC particles is more significant than the hindering effect of viscosity. However, when the SiC content further increases to 8wt%, the excessively high melt viscosity restricts the growth and movement of bubbles, resulting in smaller average cell size of the aluminum foam. The results show that increasing the SiC content improves the distribution of SiC particles in the cell wall of the aluminum foam, which enhances the film stability and facilitates the cell growth. It also increases the melt viscosity, which restricts the cell size and causes a decrease in average cell size. The average cell size of aluminum foam ultimately depends on the superposition results between the effects of melt viscosity and uniform distribution of SiC particles.

In terms of the variation of cell wall thickness, the cell walls of the aluminum foams are relatively thicker when the SiC content is less than 4wt%. This is due to the low viscosity of the melt, the relatively inferior liquid-phase film stability of the cells, and the existence of a fragile extrusion threshold for the film, which restrict the cell wall thickness decrease with the increase in viscosity. When the SiC content is 6wt%, the cell wall thickness decreases to <120 μm. At this point, the aluminum foam melt has a higher viscosity, the diffusion and expansion rates of the bubbles are balanced, and the liquid-phase film is more stable. These phenomena promote more complete foaming and more uniform cell structure distribution with good foaming stability, preventing the occurrence of cell wall collapse and deformation. As a result, the bubbles fill more space, and the cell walls become thinner. When the SiC content reaches 8wt%, it is difficult for the bubbles to diffuse and expand due to the high melt viscosity, and the tiny bubbles are aggregated in the cell wall, making it more difficult to further thin the cell walls.

3.3.2 Analysis of cell structure of aluminum foams

Fig. 8 shows the layer-by-layer porosity changes of the aluminum foams with 2wt%, 4wt%, and 6wt% SiC obtained by CT scanning. The results indicate that the porosity changes of the aluminum foam with 6wt% SiC are relatively gradual between 75%–80% with the smallest porosity difference. This aluminum foam exhibits a good cell structure, including uniform wall thickness, density, and porosity. It deforms uniformly when subjected to force, avoiding localized stress concentration and improving its strength and compressive properties. Compared with that of the aluminum foam with 6wt% SiC, the layer-by-layer porosity of the aluminum foam with 2wt% SiC has a significant decreasing trend from 84% to about 72%. The presence of multiple porous slides in the middle part indicates that the cell size variations are complex and unevenly distributed. The serious phenomena of cell missing and cell buckling lead to the material being prone to unanticipated plastic deformation and damage under stress, which reduces the overall compressive performance. The aluminum foam with 4wt% SiC has relatively high layer-by-layer porosity with small variation before the region ① in Fig. 8, but the porosity decreases sharply after entering the region ①. The aluminum foam above the red dashed line undergoes significant cell collapse and merging with the cell diameter larger than 2.5 mm and a thin cell wall. The cell diameter of air holes below the dotted red line decreases rapidly to 1.5 mm, and the cell walls become thicker. This leads to uneven density and unstable cell structure, which make the material prone to uneven deformation and breakage when subjected to force, ultimately degrading the compressive performance of the material. Combining Fig. 3, the aluminum foam with 4wt% SiC exhibits the worst cell structure, which

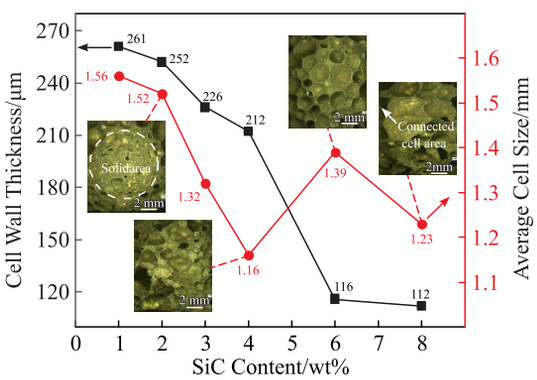

Fig.7 Variation of average cell size and cell wall thickness of aluminum foams with different SiC contents

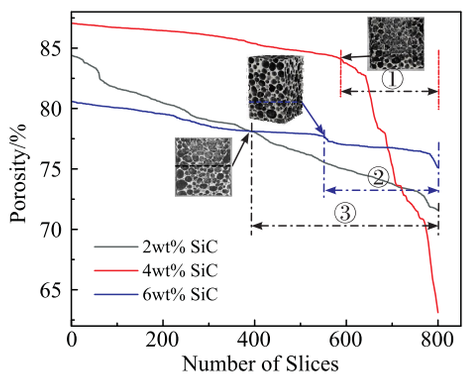

Fig.8 Layer-by-layer porosity changes of aluminum foams with different SiC contents

results from inappropriate viscosity and low viscosity, and the foaming process is more difficult to control.

Fig. 9 shows the three-dimensional wall thickness distribution cloud maps of aluminum foams with 2wt% , 4wt% , and 6wt% SiC. Among them, red represents the relatively thicker cell walls (the darker the red color, the larger the thickness); green represents uniformly thick cell walls. The results show that the wall thickness of the aluminum foam gradually increases from the center to the edge of the sidewall, where the cell diameter is smaller. In the deep red areas, many small-sized defective cells exist, and cell structure loss and curving are more serious around the edge of the sidewall than in the central part. The cell size at the bottom is smaller compared with that in the middle and upper parts. At the bottom part, the wall thickness increases, but the cell shape is more regular than that at the edge of the sidewall. With the increase in SiC content, both the sidewall and the bottom of the aluminum foam with 6wt% SiC show higher cell wall uniformity than those with 2wt% and 4wt% SiC, and the number of cell defects also decreases.

As the quantitative index of rigidity, Young's modulus represents the strength of the aluminum foam's rigidity and it is directly associated with the compressive ability. The relationship among the foam aluminum density, cell wall thickness, and Young's modulus can be expressed be Eq.(7–8), as follows:

$$E^* \approx E_{\mathrm{m}}\left(\frac{\rho^*}{\rho_{\mathrm{s}}}\right)^2 \tag{7}$$

$$\delta_{\mathrm{CE}} = E^*\left(0.86\varnothing\right)^2 \tag{8}$$

where ρ^* is the density of aluminum foam (the densities of the aluminum foams with 1wt%, 2wt%, 3wt%, 4wt%, 6wt%, and 8wt% SiC are 0.59, 0.60, 0.63, 0.65, 0.64, and 0.68, respectively); ρ_{s} is the density of the ZL102 aluminum matrix; δ_{CE} represents the contribution of the cell wall to the Young's modulus of aluminum foam; E^* is the Young's modulus of aluminum foam; $\varnothing$ is the fraction of the solid contributed by the cell wall; E_{m} is the Young's modulus of the matrix material. With the increase in SiC content, the density of aluminum foam increases slightly, and the solid fraction increases, which improves the stiffness and compressive capacity of aluminum foam. The above results indicate that the SiC content affects the wall thickness and density of aluminum foam, thereby affecting the compressive ability and rigidity.

3.4 Influence of SiC content on mechanical properties of aluminum foams

Fig. 10 shows the compressive stress-compressive strain curves of the aluminum foams with 1wt% , 2wt% , 3wt% , 4wt%, 6wt%, and 8wt% SiC. The appearances 1–4 in Fig.10 represent the aluminum foam in the uncompressed state, in the linear elastic region, in the platform deformation region, and in the densification region, respectively[32]. When subjected to pressure, the aluminum foams are compressed and the cells yield plastically, leading to a permanent change in shape in the region with lower hardness and close to the cells. As the pressure increases, the cell walls collapse and fractured fragments accumulate in the contact region, leading to a decrease in axial volume of the aluminum foam without a significant lateral expansion. During the elastic stage, the aluminum foams with different SiC contents show similar performance: they maintain a certain linear elasticity. The compressive strength (the peak stress at the end of the initial linear elastic region)[33] reaches 7.57, 8.34, 12.00, 6.48, 12.18, and 2.09 MPa when the SiC content is 1wt%, 2wt%, 3wt%, 4wt%, 6wt%, and 8wt%, respectively. Based on the enlarged compressive stress-compressive strain curves of the elastic stage, the stress reduction ratio K of the SiC aluminum foams is obtained, as indicated by the number on the curves. The calculation formula of K can be expressed as follows:

$$K = \frac{\Delta\mathrm{stress}}{\Delta\mathrm{strain}} \tag{9}$$

where Δstrain is the change in peak stress from the minimum stress; Δstress is the change in strain corresponding to the peak stress from the minimum stress[34].

As a whole, with the increase in SiC content, the compressive strength is firstly increasing and then decreasing. The compressive strength of the aluminum foam with 6wt% SiC is the highest, whereas that of the aluminum foam with 8wt% SiC is the lowest. The aluminum foam with 4wt% SiC does not conform to the regular change because it has the critical value of viscosity. The stress reduction ratio is larger for the aluminum foams with high SiC content. The abovementioned phenomena are attributed to the fact that the high-hardness SiC particles are embedded in the softer aluminum matrix, forming a high-strength skeleton that increases the compressive strength of the aluminum foam. In addition, the uniformly dispersed SiC particles can effectively hinder the dislocation slip within the matrix; the interactions

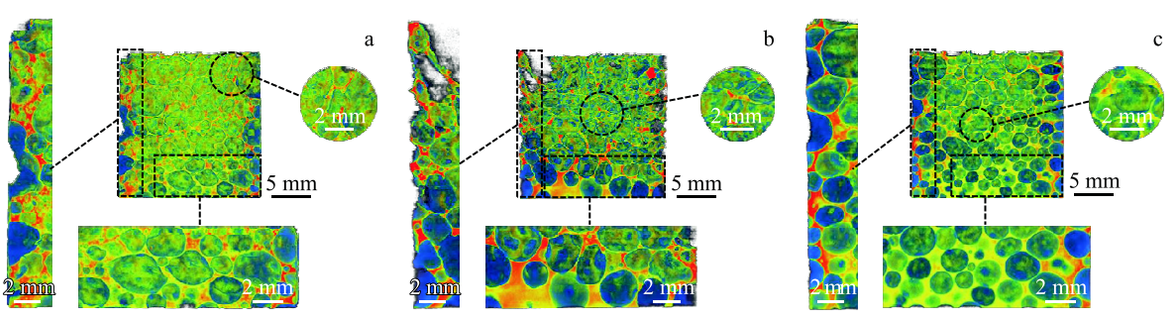

Fig.9 Three-dimensional wall thickness distributions of aluminum foams with different SiC contents: (a) 2wt%, (b) 4wt%, and (c) 6wt%

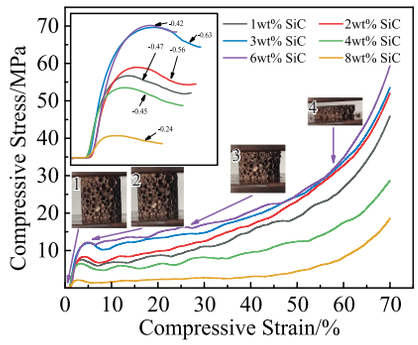

Fig.10 Compressive stress-compressive strain curves of aluminum foams with different SiC contents

between the SiC particles and the aluminum matrix are promoted; the growth of microcells will be hindered, further reducing the number and size of microcells, and improving the deformation resistance of the material. When the material is subjected to pressure, the stress can be better dispersed to avoid material rupture due to stress concentration. However, too high SiC content (8wt%) leads to the formation and uneven distribution of large-sized SiC particles (Fig. 4f), which destroys the cell structure of the aluminum foam and leads to a decrease in compression properties. Therefore, the SiC particles play a crucial role in optimizing the strength of the aluminum matrix, and the strength of the aluminum foam is increased with the increase in SiC content. But it is necessary to control the SiC content to prevent the destruction of the cell structure. Insufficient or excessive SiC particles may lead to the depreciation of the material properties, which results in the deterioration of the compressive properties of the aluminum foam.

Fig.11 shows the energy absorption curves of the aluminum foams with different SiC contents. As a whole, the aluminum foam with 6wt% SiC has the optimal energy absorption effect with a total absorption of 1369.68 J/mm^3. The aluminum foam with 8wt% SiC has the worst energy absorption effect with the total absorption of only 226.9 J/mm^3. This result is consistent with the abovementioned research results. When the deformation amount reaches 60%–70%, the aluminum foam is subjected to its limit strain, achieving densification and

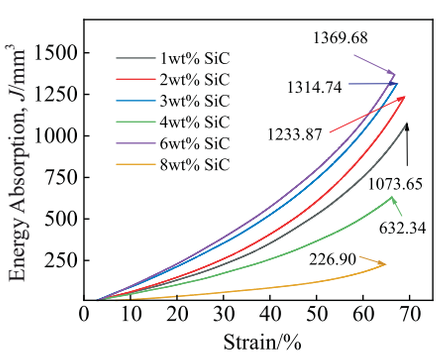

Fig.11 Energy absorption curves of aluminum foams with different SiC contents

thereby causing the rise of the stress-strain curves. The slope value tends towards E_s value. The maximum value is the energy absorption, which can be expressed as ε_D[35], as follows:

$$\varepsilon_D = 1 - 1.4\left(\frac{\rho^*}{\rho_s}\right) \quad (10)$$

The results indicate that during the preparation of aluminum foams, the amount of SiC addition needs to be appropriately controlled to regulate the microscopic properties, such as matrix strength, and macroscopic structures, such as cell diameter and cell wall thickness, to comprehensively optimize the compressive strength of aluminum foams.

4 Conclusions

1) An appropriate increase in SiC content improves the foaming stability and ameliorates the cell structure, resulting in thin-walled and uniform cells. Meanwhile, the compressive strength and Vickers hardness of the aluminum foams are improved. High SiC content (>4wt%) leads to higher stress reduction ratio.

2) The aluminum foam with 6wt% SiC has suitable viscosity state and exhibits the optimal particle distribution uniformity, foaming stability, and cell structure features. When the aluminum foam is subjected to stress, the uniform wall thickness and cell distribution can avoid the stress concentration, which results in the strongest compressive capacity and absorbed energy of 1369.68 J/mm^3.

3) The aluminum foam with 4wt% SiC is in the transition state, lacks the characteristics of low-viscosity aluminum foam, and partly exhibits the properties of suitable-viscosity aluminum foam. It is complicated and challenging to control cell structure of the aluminum foam with 4wt% SiC. Besides, the aluminum foam with 8wt% SiC is in a high viscosity state, exhibiting particle clustering behavior, serious cell structure damage, and poor uniformity. Although the states of the aluminum foams with 4wt% and 8wt% SiC are different, they both ultimately show inferior mechanical properties.

4) The aluminum foams with 1wt%–3wt% SiC are in the low viscosity state, their cell structure is relatively good, but the foaming stability is inferior, and the preparation process is difficult to control.

References

1 Garai F, Béres G, Weltsch Z. *Materials Science and Engineering A*[J], 2020, 790: 139743

2 Sunder S S, Yadav S, Joshi A *et al*. *Materials Today: Proceedings*[J], 2022, 63: 347

3 Zhang Y, Pan R, Xiao F. *International Journal of Distributed Sensor Networks*[J], 2020, 16(11): 15501477209

4 Wang Z, Zhang Z, Liu N N *et al*. *Rare Metal Materials and Engineering*[J], 2024, 53(3): 667

5 García-Moreno F. *Materials*[J], 2016, 9(2): 85

6 Fu W, Li Y. *Materials*[J], 2024, 17(3): 560

7 Wang H, Zhu D F, Hou S *et al*. *Materials and Design*[J], 2020, 196: 109090

8 Shang J T, Xuming C, Deping H. *Materials Science and Engineering B*[J], 2008, 151(2): 157

9 Wang H, Zhang Y M, Zhou B C *et al*. *Journal of Materials Science and Technology*[J], 2016, 32(6): 509

10 Wang Deqing, Shi Ziyuan. *Materials Science and Engineering A*[J], 2003, 361(1–2): 45

11 Babcsán N, Leitlmeier D, Degischer H P *et al*. *Advanced Engineering Materials*[J], 2004, 6(6): 421

12 Babcsán N, Leitlmeier D, Degischer H P. *Materials Science and Engineering Technology*[J], 2003, 34(1): 22

13 Heim K, García-Moreno F, Banhart J. *Scripta Materialia*[J], 2018, 153: 54

14 Wübben T, Odenbach S. *Colloids and Surfaces A: Physicochemical and Engineering Aspects*[J], 2005, 266(1–3): 207

15 Lin H, Luo H, Huang W *et al*. *Journal of Materials Processing Technology*[J], 2016, 230: 35

16 Kumar G S V, Heim K, Mukherjee M *et al*. *Materials Today Communications*[J], 2024, 38: 108257

17 Sasikumar S, Georgy K, Mukherjee M *et al*. *Materials Letters*[J], 2020, 262: 127142

18 Sinha A A, Mondal D P, Muchhala D *et al*. *Journal of Materials Engineering and Performance*[J], 2022, 32(14): 6248

19 Mudge A, Morsi K. *Metals*[J], 2024, 14(1): 120

20 Papantoniou I G, Manolakos D E. *The International Journal of Advanced Manufacturing Technology*[J], 2024, 130(11–12): 5359

21 Thulasikanth V, Padmanabhan R. *Materials Today: Proceedings*[J], 2021, 46: 1437

22 An Y, Ma H, Zhang J *et al*. *Journal of Materials Processing Technology*[J], 2021, 296: 117212

23 An Y, Deng B, Ma H *et al*. *Journal of Materials Research and Technology*[J], 2024, 29: 1321

24 Deng F, Liu Y, Lu X *et al*. *Metals and Materials International*[J], 2019, 26(10): 1596

25 Haibel A, Rack A, Banhart J. *Applied Physics Letters*[J], 2006, 89(15): 154102

26 Song Z L, Ma L Q, Wu Z J *et al*. *Journal of Materials Science*[J], 2000, 35(1): 15

27 Wang T, Zuo X, Yi J *et al*. *Journal of Materials Research and Technology*[J], 2024, 33: 5708

28 Huo S, Xie L, Xiang J *et al*. *Applied Physics A*[J], 2018, 124(2): 209

29 Yang Z, Li Z, Zhang L. *Materials Science and Engineering A*[J], 2024, 903: 146643

30 Kota N, Jana P, Sahasrabudhe S *et al*. *Materials Today: Proceedings*[J], 2021, 44: 2930

31 Wang T, Zuo X, Zhou Y *et al*. *Journal of Materials Research and Technology*[J], 2021, 11: 1991

32 Dehnavi A, Ebrahimi G R, Golestanipour M. *Journal of the Brazilian Society of Mechanical Sciences and Engineering*[J], 2020, 42(11): 554

33 Zhang B, Lin Y, Li S *et al*. *Composites Part B: Engineering*[J], 2016, 98: 288

34 Ferguson J B, Santa M J A, Schultz B F *et al*. *Materials Science and Engineering A*[J], 2013, 582: 423

35 Wan T, Liu Y, Zhou C *et al*. *Journal of Materials Science and Technology*[J], 2021, 62: 11

SiC 含量对两步发泡法制备的SiC/Al基复合泡沫的发泡稳定性、孔结构和压缩性能的影响

黄闻战，刘　涛，陈　尧，王录才，武建国，游晓红

(太原科技大学 材料科学与工程学院，山西 太原 030024)

摘　要：采用两步发泡法制备了SiC/Al基复合泡沫。研究了SiC含量及其分布均匀性对泡沫铝的发泡稳定性、孔结构和力学性能的影响，对泡沫铝的宏观/微观特征进行了表征和分析。结果表明，适当增加SiC的含量并使SiC分布均匀，可以提高泡沫铝的发泡稳定性，优化孔径和孔壁厚度的大小以及孔的分布，增强泡沫铝的硬度和抗压缩强度。然而，SiC含量不足或过多都会导致SiC颗粒分布不均，不利于发泡稳定性和良好孔结构的形成。当SiC含量为6wt%时，泡沫铝的发泡稳定性和孔结构都达到了最佳状态，从而获得了最高的压缩强度和最佳能量吸收能力。

关键词：泡沫铝；两步发泡法；发泡稳定性；孔结构；硬度；压缩强度

作者简介：黄闻战，男，1989年生，博士，教授，太原科技大学材料科学与工程学院，山西 太原 030024，E-mail：2019063@tyust.edu.cn